

DESIGN, FABRICATION, *IN VITRO*, AND *EX-VIVO* PERMEATION STUDY OF MICRO-EMULSIFIED HYDROGEL OF FLUCONAZOLE (MHG-FLCZ) USING A CENTRAL COMPOSITE DESIGN (CCD)

SOUMYADIP GHOSH^{1*}, ANKITA BASAK¹, DEBGOPAL GANGULY², ANKITA POREY³

¹Department of Pharmaceutics, Bengal School of Technology (A College of Pharmacy), Delhi Rd, Chinsurah RS, Sugandha, West Bengal-712102, India. ²Burdwan Institute of Pharmacy, Bhatchala, Sripally, Purba Bardhaman-713103, India. ³Department of Pharmaceutical Chemistry, Secom Pharmacy College, Dhulagori, Howrah-711313, West Bengal, India
*Corresponding author: Soumyadip Ghosh; Email: soumyadeep271@gmail.com

Received: 15 Nov 2023, Revised and Accepted: 28 Dec 2023

ABSTRACT

Objective: The current study's objective was to develop and characterize a micro-hydrogel-based fluconazole (FLCZ) gel. A micro-hydrogel (Mhg) was prepared using different concentrations of Carbopol 940 (CP) and NaCMC using the modified swelling hydrogel method.

Methods: A Preformulation study was performed using FTIR to confirm the drug and polymers were compatible with each other based on the functional group determination. 3² optimization procedures were used to develop formulations based on the response surface methodology. The prepared formulations were evaluated for entrapment efficiency, spreadability, viscosity, and visual examination using binocular microscopy and *in vitro* drug release using Franz diffusion cells.

Results: The optimized formulation F2 reported entrapment efficiency of 65.09±0.41%, and viscosity of 11100±1.21 cps. The *in vitro* release of drug for the prepared formulations was performed for 8 h. and the optimized formulation showed better-controlled drug release compared to other formulations. It was observed that the optimized batch, percentage of drug permeability through the skin at 8 h of ex-vivo study shows 84.67±0.67% and *in vitro* drug release study (93.22%) through Franz diffusion cell, which suggests that the drug (Optimum batch) can easily penetrate through the skin and showed the highest drug release in a stipulated time interval.

Conclusion: The use of an optimized Mhg-FLCZ gel formulation as it has excellent homogeneity, a pH that is close to that of the skin, and suitable thixotropic characteristics relates to that much more convenience than the conventional dosage form. The *in vitro* and ex-vivo study data proved its suitability as a better alternative to conventional products in the effective treatment of skin infections.

Keywords: Fluconazole, Hydrogel, Topical drug delivery, Optimization, Fungal infection and microemulsion

© 2024 The Authors. Published by Innovare Academic Sciences Pvt Ltd. This is an open access article under the CC BY license (<https://creativecommons.org/licenses/by/4.0/>)
DOI: <https://dx.doi.org/10.22159/ijap.2024v16i2.49865> Journal homepage: <https://innovareacademics.in/journals/index.php/ijap>

INTRODUCTION

Targeting the drug delivery system to the topical route is much more prominent in delivering the dosage form to avoid first-pass metabolism, enzyme degradation by the gastrointestinal tract, and improved patient compliance [1]. Topical formulations are smeared, rubbed, sprayed, or instilled directly onto the external body surface. Both local and systemic medication effects have been produced by using the topical route of administration to treat skin diseases [2, 3]. Fluconazole (FLCZ), an antifungal agent belonging to the azole group of drugs interacts with the enzymes responsible for ergosterol synthesis which alters the cell membrane fluidity. This micro-hydrogel improves drug solubility and facilitates drug absorption across the skin in comparison to the traditional topical preparation [4]. The gel is emollient, promptly spreadable, quickly removed, non-staining, and readily compatible with several types of excipients. An essential feature of gel systems is the structural network formed by polymers. Gel formulations show variation with the variability of polymer type and concentration, which affect drug release [5]. The term micro-emulsified hydrogel (Mhg) describes thermodynamically stable, fluid, translucent, or transparent homogenous dispersions composed of the oil phase, aqueous phase, surfactant, and co-surfactant in the appropriate ratios, a single optically isotropic in nature dispersion with a droplet diameter usually in the 10-100 micrometer range is generated [6]. Micro-hydrogel (Mhg) is far superior to conventional formulations because it enhances drug solubility, is easier to manufacture, and is more effective at delivering drugs transdermally [7].

The current study's objective was to design and characterize a micro-emulsified hydrogel of fluconazole (Mhg-FLCZ) using a central composite design (CCD). In order to formulate a Mhg-FLCZ, carbopol 940 (CP) and sodium carboxymethyl cellulose (NaCMC) at different concentrations were used. 3² optimization techniques were used to develop formulations based on the response surface

methodology. The prepared formulations were investigated to determine the optimized formulation as entrapment efficiency, spreadability, viscosity, and visual examination using binocular microscopy, *in vitro* drug release, and *ex-vivo* permeation study using Franz diffusion cells.

MATERIALS AND METHODS

Material

Fluconazole drug was gifted from Cipla, Sikkim, India. Carbopol 940 was purchased from Sigma Aldrich, America. Sodium carboxy methyl cellulose (NaCMC) and Glycerine were purchased from Sigma Chemical Corporation Pvt. Ltd. Other than that, all of the chemicals and reagents used in the studies followed pharmaceutical standards and were of analytical quality.

Fabrication of Mhg-FLCZ

All 9 formulations of FLCZ topical gel were prepared using different concentrations of Carbopol 940 (CP) and NaCMC using the modified swelling hydrogel method [8, 9]. The composition of different formulations of Mhg-FLCZ is presented in table 1. CP and NaCMC were soaked overnight at different concentrations. The organic phase was prepared using a drug (FLCZ) dissolved in 10 ml of methanol and glycerin. Organic phase transfer drop by drop through a micropipette to an aqueous phase containing CP and NaCMC makes oil in water (o/w) using a magnetic stirrer with the speed of 8000 rpm. Alcohol (methanol) was utilized to improve penetration while glycerin served as a moisturizing ingredient. Allow to hydrate and swell slowly addition of methyl paraben and propyl paraben sodium under stirring of 8000 rpm. To adjust the skin pH, triethanolamine was used and the content was overnight at room temperature to get a homogenous gel of Mhg-FLCZ.

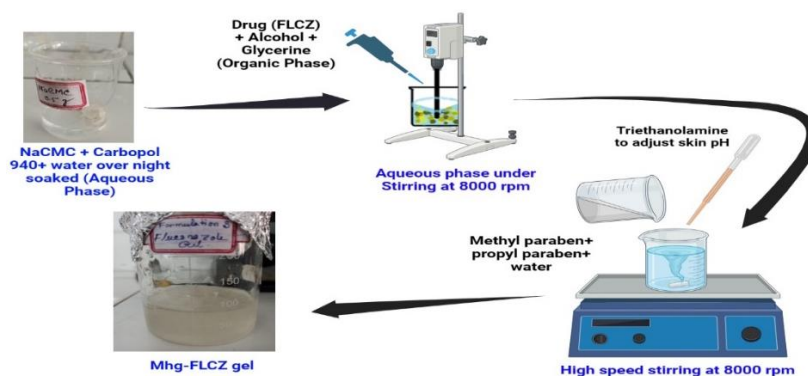


Fig. 1: Preparation of Mhg-FLCZ using the modified swelling hydrogel method

Table 1: Formulation table of Mhg-FLCZ

F. No	FLCZ (mg)	CP (%w/v)	NaCMC (%w/v)	Glycerine (ml)	Triethanolamine (ml)	Methyl paraben sodium (%w/v)	Propyl paraben sodium (%w/v)
F1	100	1.5 (+1)	1.0 (0)	10	0.3	0.1	0.05
F2	100	0.5 (-1)	1.0 (0)	10	0.3	0.1	0.05
F3	100	0.5 (-1)	1.5 (+1)	10	0.3	0.1	0.05
F4	100	1.5 (+1)	1.5 (+1)	10	0.3	0.1	0.05
F5	100	1 (0)	0.5 (-1)	10	0.3	0.1	0.05
F6	100	1.5 (+1)	0.5 (-1)	10	0.3	0.1	0.05
F7	100	1 (0)	1.0 (0)	10	0.3	0.1	0.05
F8	100	0.5 (-1)	0.5 (-1)	10	0.3	0.1	0.05
F9	100	1 (0)	1.5 (+1)	10	0.3	0.1	0.05

Characterization of Mhg-FLCZ

Entrapment efficiency (%) of Mhg-FLCZ

The concentration of free drug in the dispersion medium was measured in order to assess the entrapment efficiency (%) of different formulations of Mhg-FLCZ. 10 µg/ml diluted solution of Mhg-FLCZ was prepared using phosphate buffer 7.4 and poured onto Whatman filter paper with a pore size range of 0.22 µm and collected the filtrate. At 260 nm, the absorbance of the solution was measured using a spectrophotometer (Shimadzu 1800). The equation entrapment efficiency (%) was used to calculate the entrapment efficiency of Mhg-FLCZ [12].

$$\text{Entrapment efficiency (\%)} = \frac{\text{Amount of drug used in the formulation} - \text{Amount of untrapped drug}}{\text{Amount of the drug used in the formulation}} \times 100$$

pH of Mhg-FLCZ

Mhg-FLCZ of each gel formulation was transferred to 10 ml of the beaker and measured by using the digital pH meter (Remi, India). pH of the topical gel formulation should be between 3–9 to treat the skin infections [13].

Spreadability of Mhg-FLCZ

Two slides (split into squares with 5 mm sides) were used to press a sample of 0.5 g of each formula between them. and when no further spreading was anticipated, left for around five minutes. The spread circle diameters were measured in centimeters and used as standards for spreadability [14].

Viscosity of Mhg-FLCZ

A Brookfield viscometer DVII model with a T-Bar spindle and helipath stand was used to determine gel viscosity. All Mhg-FLCZ gels were measured using Spindle T 95. T95, the T-bar spindle, was lowered perpendicularly to ensure that it wouldn't contact the bottom of the jar and measure the viscosity of Mhg-FLCZ formulations [15].

Measurement of viscosity of Mhg-FLCZ

Several factors impact this, such as sample size, sample pressure, and

temperature. Viscosities were measured at several locations along the helipath by moving the T-bar spindle up and down [16]. The torque value was consistently higher than 10%. The viscosity of gels was determined by taking an average of three readings in a minute [17, 18].

FT-TR (Fourier transform infra-Red)

Fourier transform infrared spectroscopy (Perkin Elmer, America) was used to analyze the drug's interaction with the polymers of Mhg-FLCZ. FLCZ IR absorption peak was measured between 400 and 4000 cm⁻¹, utilizing the KBr disc approach [19]. For the purpose of evaluating purity, the primary peak was reported [20].

Visual examination of Mhg-FLCZ

To determine the surface of the particles of Mhg-FLCZ using a binocular microscope (Labomed LX-300). Using binocular microscopy at different magnification ranges as 1000x and 1500x to analyze the morphology and size uniformity of Mhg-FLCZ [21, 22].

In vitro release profile of Mhg-FLCZ

The Franz diffusion cell instrument (Orchid Scientific EMFDC-06, India) was used to conduct *in vitro* diffusion investigations [23, 24]. Dialysis membrane with a molecular weight cut off of 12000 to 14000 Da from Hi-Media Laboratories Pvt. had a receptor compartment capacity of 20 ml and a donor compartment exposure area of 1.41 cm. Dialysis membrane has a flat width of 24.26 mm and a diameter of 14.3 mm with an approximate capacity of 1.61 ml/cm was used for the study. The membrane was soaked overnight in phosphate buffer pH 7.4. 10 ml of prepared Mhg-FLCZ (containing phosphate buffer), which contains 10 mg FLCZ was taken and placed in the donor cell. A dialysis membrane was placed in between the donor cell and the receptor cell. 20 ml of phosphate buffer (pH 7.4) was taken in the receptor cell to touch the bottom surface of the dialysis membrane. The temperature of the receptor phase was maintained at 37±0.5 °C and the receptor compartment was stirred with a magnetic stirrer to maintain a homogeneous condition. The aliquots of 1 ml were withdrawn at different time intervals. Fresh medium was used to replace an equal volume of the sample withdrawn. The samples were analyzed at 260 nm in a UV-visible spectrophotometer (Shimadzu 1800) and the amount of drug

released at different time intervals was calculated. *In vitro* analyses were performed for 8 h. Numerous kinetic studies, including first order, zero order, Korsmeyer-Peppas model, and Higuchi's model, were carried out to ascertain the manner and mechanism of Mhg-FLCZ release from various formulations.

Ex-vivo permeation study of Mhg-FLCZ

The optimized formulation was tested for permeation in *ex-vivo* using Franz's diffusion cell (Orchid Scientific EMFDC-06, India), which has a 3.14 cm² diffusion area. This research used rat abdominal skin for the permeation. The receptor compartment was pointed towards the dermis, whereas the donor compartment was pointed towards the stratum corneum of the excised rat skin. The donor compartment was filled with Mhg-FLCZ gels, and the receptor compartment was filled with 20 ml of medium [25, 26].

On the receptor side of the experiment, Teflon-coated magnetic beads were used to stir the solution at 50 rpm while maintaining it at 37±0.5 °C. Following the injection of the test formulation on the donor side, at predetermined intervals of 1, 2, 4, 6, and 8 h, to maintain the sink condition, 1 ml of samples were taken from the receiver compartment and after each sample was taken, an equal volume of receptor fluid was injected into the receiver compartment. Using a UV-visible spectrophotometer with a maximum wavelength of 260 nm, this study assessed the amount of Mhg-FLCZ gel in receptor fluids [27, 28].

Statistical design

As two independent variables, the amounts of carbopol 940 (A) and NaCMC (B) were varied at three levels: low (-1), medium (0), and high (+1). Performance in a factorial design (two factors and three levels) was used to modify the Mhg-FLCZ for best performance. Different levels of independent variables that are taken into consideration during the Mhg-FLCZ optimization process were applied to the trial batch's operation. There are three separate dependent or response variables: entrapment efficiency (%) (Y1), viscosity (cps) (Y2), and percentage (%) of drug release at 8 h (Y3). Throughout the optimization process, these were taken into consideration. The trial version of Design Expert 11 was used to generate and analyze experimental data. The independent and dependent variable designs are shown in table 2.

The Mhg-FLCZ was developed based on the optimization of independent variables on dependent variables by the application of a polynomial equation with parameters such as independent factors and interaction with observed responses, which were taken into consideration in the research [30, 31].

$$Y = b_0 + b_1 A + b_2 B + b_3 AB + b_4 A^2 + b_5 B^2$$

In the present evaluation, the dependent variable was Y, the intercept value was b₀, the regression coefficients employed were b₁, b₂, b₃, and b₅, and the response factors were A and B. AB is thought to represent an interaction between the variables A and B. One-way ANOVA was used to determine the significance of the models (p<0.05) and individual response parameters. Entrapment efficiency (%) (Y1), viscosity (cps) (Y2), and percentage (%) of drug release at 8 h (Y3) were shown to preserve the best response acceptability.

Statistical analysis

With the support of GraphPad Prism 5.0 (GraphPad Software, Inc., San Diego, CA, USA), the data was analyzed and reported as mean (SD). The formulation was optimized using the trial version of Design Expert Software, Version 13.0. A difference below the probability threshold of a P-value of 0.05 was determined using ANOVA.

RESULTS AND DISCUSSION

Formulation optimization

The quadratic model is used to identify how to analyze individual primary components and interaction factors utilizing the design expert program (Design Expert 11, State Ease Inc., USA). 3² full-factorial designs were used to optimize the various examined responses, each of which is represented by a quadratic as follows. The amount of CP (A) and amount of NaCMC (B) were utilized as independent variables in this full factorial design based on responses from multiple trial batches and changed at three different levels: low (-1), medium (0), and high (+1). Entrapment efficiency (%), Viscosity (cps), and percentage (%) of drug release at 8 h are the three separate response variables. The quadratic model was used to identify how to analyze individual primary components and interaction factors using the design expert software (Design Expert 11, Stat Ease Inc., USA). Using a quadratic equation, the various explored responses are indicated as follows.

Table 2: Experimental methodology of 3² factorial layouts with actual responses for various Mhg-FLCZ formulations (coded values in brackets)

Formulary indication	Factors used at the various levels		Responses*		
	Carbopol 940 (%w/v) (A)	NaCMC (%w/v) (B)	Entrapment efficiency* (%)	Viscosity (cps)*	% Drug release at 8 h (%)
F1	1.5 (+1)	1.0 (0)	52.83±0.64	7600±3.15	56.82
F2	1.5 (+1)	1.5 (+1)	65.09±0.41	11100±1.21	93.22
F3	0.5 (-1)	1.5 (+1)	46.93±0.64	4900±3.44	77.86
F4	0.5 (-1)	1.0 (0)	45.05±0.69	4000±2.65	65.88
F5	1 (0)	0.5 (-1)	36.32±0.71	3800±1.67	43.67
F6	1.5 (+1)	0.5 (-1)	47.64±0.61	5200±1.88	70.60
F7	1 (0)	1.0 (0)	46.93±0.41	4500±3.55	60.22
F8	0.5 (-1)	0.5 (-1)	36.08±0.32	3400±1.89	78.82
F9	1 (0)	1.5 (+1)	48.58±0.22	6500±2.26	72.04

*mean±Standard Deviation; n = 6.

Table 3: ANOVA summary for the response surface quadratic model of entrapment efficiency (%), Viscosity, and percentage (%) drug release at 8 h

Response 1: Entrapment efficiency						
Source	Sum of squares	df	Mean square	F-value	p-value	
Model	573.80	5	114.76	12.85	0.0307	significant
A-Drug: Polymer	234.37	1	234.37	26.24	0.0144	
B-%NaCMC	274.19	1	274.19	30.69	0.0116	
AB	10.89	1	10.89	1.22	0.3502	
A ²	49.87	1	49.87	5.58	0.0992	
B ²	4.48	1	4.48	0.5015	0.5299	
Residual	26.80	3	8.93			
Cor Total	600.60	8				

Response 2: Viscosity						
Source	Sum of squares	df	Mean square	F-value	p-value	
Model	4.70907	5	9.41906	66.23	0.0029	significant
A-Drug: Polymer	2.24307	1	2.24307	157.69	0.0011	
B-%NaCMC	1.70007	1	1.70007	119.54	0.0016	
AB	4.84006	1	4.84006	34.03	0.0100	
A ²	2.42006	1	2.42006	17.02	0.0258	
B ²	4.05005	1	4.05005	2.85	0.1901	
Residual	4.26705	3	1.42205			
Cor Total	4.75207	8				

Response 3: Drug release at 8 h						
Source	Sum of squares	df	Mean square	F-value	p-value	
Model	7.22	5	1.44	118.51	0.0012	significant
A-Drug: Polymer	3.79	1	3.79	311.23	0.0004	
B-%NaCMC	2.86	1	2.86	234.45	0.0006	
AB	0.4830	1	0.4830	39.64	0.0081	
A ²	0.0868	1	0.0868	7.12	0.0757	
B ²	0.0011	1	0.0011	0.0894	0.7845	
Residual	0.0366	3	0.0122			
Cor total	7.26	8				

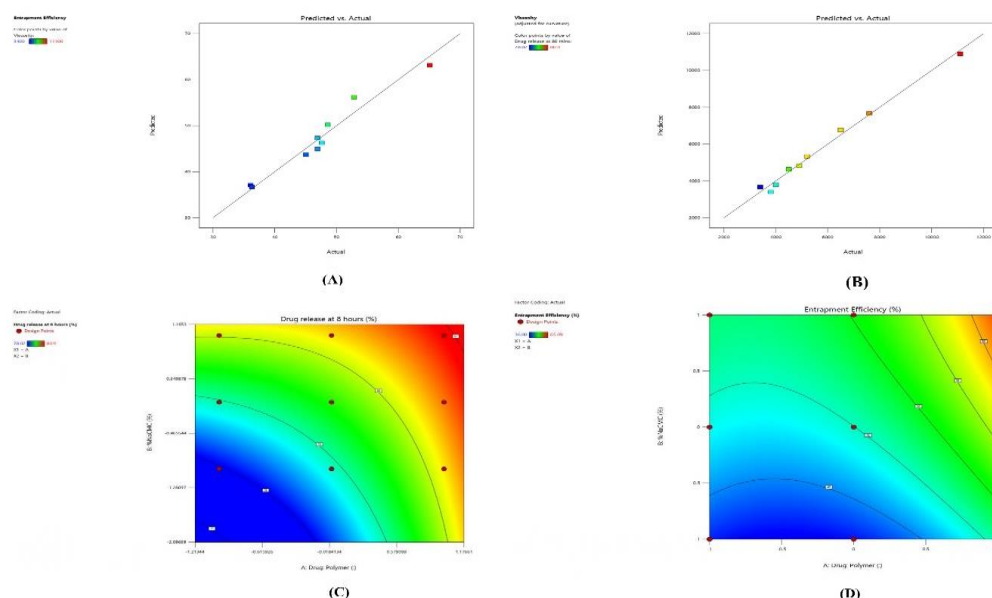


Fig. 2: (A) An analysis of % Entrapment efficiency between actual and predicted values is illustrated in this linear correlation plot. (B) A linear correlation plot is shown between the actual and predicted viscosity of Mhg-FLCZ. (C) Comparison of the actual and predicted release of % of drug at 8 h shown in a linear correlation plot. (D) Contour plot demonstrating the amount of CP (A) and % w/v NaCMC (B) affect the percentage of entrapment efficiency (%)

Entrapment Efficiency (EE%) = $44.94 + 6.25A + 6.76B + 1.65AB + 4.99A^2 - 1.49B^2$ [$R^2 = 0.9554$; F value = 12.85; $P < 0.05$]

Viscosity = $4633.33 + 1933.33A + 1683.33B + 1100AB + 1100A^2 + 450B^2$ [$R^2 = 0.991$; F value = 66.23; $P < 0.05$]

Drug Release at 8 h = $79.55 + 0.795A + 0.69B - 0.3475AB + 0.20833A^2 + 0.0233B^2$ [$R^2 = 0.9952$; F value = 118.51; $P < 0.05$].

The high correlation coefficient (R^2) value from the aforementioned model equations shows that the variables under investigation have a significant influence on the investigated responses. The ANOVA results (table 3) clearly showed that both factors—the quantity of CP and the percentage of w/v NaCMC—had significant ($p < 0.05$) impacts on drug release at 8 h (%), viscosity (cps), and entrapment efficiency (%). Eliminating the non-significant ($p > 0.05$) components allowed for model reduction of the above-mentioned quadratic equations.

Fig. 2A shows linear correlation graphs comparing the actual and expected findings, as well as residual plots linking entrapment efficiency (%), viscosity (cps), and drugs released at 8 h (%). The corresponding residual plots showing the scatter of the observed

versus predicted values relating to entrapment efficiency (%), viscosity (cps), and drug released at 8 h (%). are presented in fig. 2 (A), 2 (B) and 2 (C), respectively. The influence of both independent variables (The amount of CP and % w/v of NaCMC) on investigating responses (entrapment efficiency (%), viscosity (cps), drug released at 8 h (%)) was further explicated using two-dimensional contour plots and three-dimensional response surface plots.

The contour plot relating entrapment efficiency in fig. 2 (D) depicted the non-linear decrease of entrapment efficiency (%) with an increase in % w/v of NaCMC. However, the entrapment efficiency (%) was linearly increased with an increase in the amount of the amount of CP (A). At low and high levels of B, entrapment efficiency was significantly ($p < 0.05$) increased when the amount of CP (A) increased from -1 level to +1 level. The response surface plot relating entrapment efficiency (%) (fig. 3 (C)) indicated that the entrapment efficiency (%) was more dependent upon the amount of CP (A) compared to the % w/v of NaCMC (B). The response surface plot also showed the strip-linear curvature on the axis of the amount of CP (A), while an almost flattening curve was seen for the % w/v of NaCMC (B).

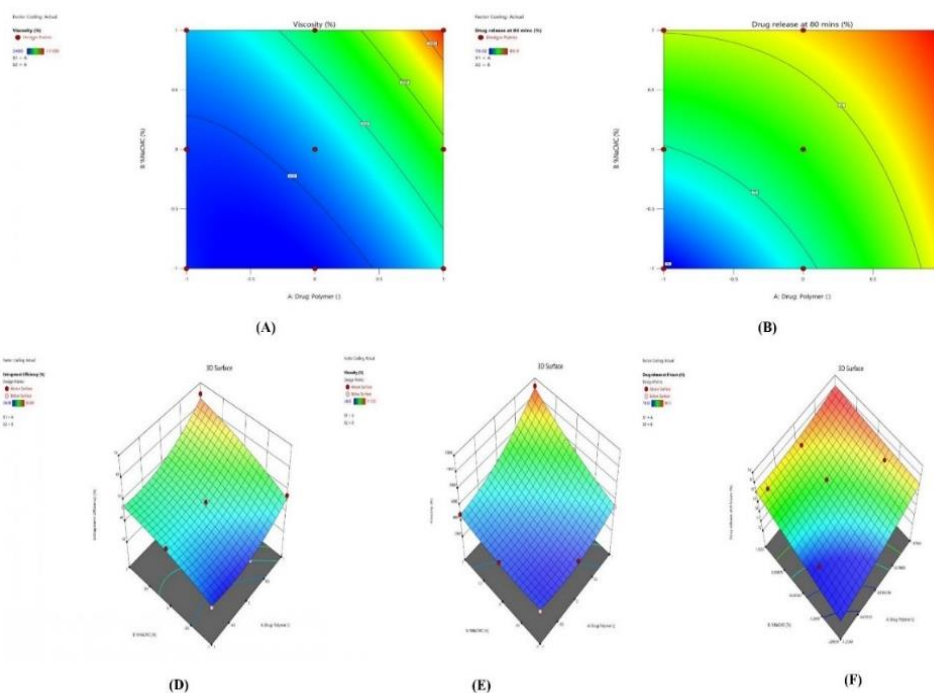


Fig. 3: (A) Contour plot demonstrating the impact of the amount of CP (A) and % w/v NaCMC (B) ratio on the Mhg-FLCZ viscosity. (B) Contour plot demonstrating the impact of the amount of CP (A) and % w/v NaCMC (B) on the ratio of the Mhg-FLCZ drug release at 8 h. (C) Response Surface plot demonstrating the amount of CP (A) and % w/v NaCMC (B) ratio on the entrapment efficiency (%) of Mhg-FLCZ. (D) Response Surface plot demonstrating the amount of CP (A) and % w/v NaCMC (B) ratio on the viscosity (cps) of Mhg-FLCZ. (E) Response Surface plot demonstrating the amount of CP (A) and % w/v NaCMC (B) ratio on the % drug release at 8 h of Mhg-FLCZ

The contour plot illustrates the viscosity (cps) in fig. 3 (A). The amount of CP and B (% w/v of NaCMC) showed a linear increase in entrapment efficiency (%) with an increase in the amount of CP (A) and %W/V of NaCMC (B). At a low level (-1) of % w/v of NaCMC (B), the viscosity (cps) was significantly ($p < 0.05$) increased when the amount of CP (A) increased from -1 level to +1 level. Moreover, a similar result was observed on the viscosity (cps), A was increased from -1 level to +1 level at a high level of B (+1). The response surface plot relating viscosity (cps) (fig. 3 (D)) designated the slightly linear curvature on the axis of the amount of CP (A) and %w/v of NaCMC (B). This indicated that both the amount of CP (A) and % w/v NaCMC (B) had a considerable effect on viscosity (cps).

The contour plot (fig. 3 (B)) of the drug released at 8 h (%) versus factors A and B despite the linear increase of drug released at 8 h with an increase in the amount of % w/v NaCMC (B). On the other hand, a non-linear slight increment of drug released at 8 h (%) was observed with an increased amount of CP (A). At low and high levels of A, the drug released at 8 h (%) was significantly ($p < 0.05$) increased as B was increased from -1 level to +1 level. This designated that the amount of % w/v NaCMC (B) had pronounced effects on the drug released at 8 h (%) as compared to the amount of CP (A).

According to the equation above, a high correlation coefficient value indicates that the experiment's components and the analyzed responses are closely related. According to the ANOVA result, both of the factors, the amount of CP (A) and % w/v NaCMC (B) had a significant effect on drug entrapment efficiency (%), viscosity, and percentage (%) drug release at 8 h, with a p-value of 0.05 or below. The quadratic model's simplicity was seen as a key concept.

Entrapment efficiency (EE%)

The entrapment efficiency (%) of various Mhg-FLCZ is presented in table 2. entrapment efficiency (%) of Mhg-FLCZ was found within the range of $36.08 \pm 0.32\%$ to $65.09 \pm 0.41\%$. The poor entrapment

efficiency (%) of Mhg-FLCZ might be low solubility and poor lipophilicity. It has been reported that the microparticles are capable of reducing drug leakage, prolonging the residence time of the drug on the skin, and facilitating the internalization of drugs into cells. The entrapment efficiency (%) was found significantly ($p < 0.05$) increased as the amount of CP and % w/v of NaCMC were increased.

pH of Mhg-FLCZ

Triethanolamine was used in small quantities in all batches (F1-F9) to maintain the pH close to the skin's (5.6). All batches have pH values ranging from 4.1 ± 0.18 to 5.6 ± 0.28 . To prevent skin irritation and other associated issues, Mhg-FLCZ gel formulations should have a pH value adjusted to be close to that of the skin [32]. The pH and viscosity of hydrogel thickened microemulsion gradually increased with a decrease in concentration of surfactant co-surfactant mixture in the formulation.

Spreadability

Spreadability tests were performed for all formulations, and for the Mhg-FLCZ gel formulation, the spreadability of the gel formulation reduced as the polymer concentration increased. The spreadability range of the Mhg-FLCZ was found to be 1.28 ± 0.04 g. cm/s to 3.6 ± 0.01 g. cm/s. Spreadability is the term utilized to describe a cream's ability to spread over the skin. Spreadability is essential because it explains the way gel behaves when it escapes from the tube. As a topical cream gets closer to the skin's surface, its ability to spread decreases [33].

Viscosity

Table 2 displays the viscosity for various Mhg-FLCZ formulations. The viscosity of Mhg-FLCZ was found within the range of 3400 ± 1.89 cps to $1,11,00 \pm 1.21$ cps. Low quantities of A and low amounts of B show that the gel's physical strength has decreased due to a decrease in viscosity. The viscosity was found significantly ($p \leq 0.05$) increased as the amount of CP and % w/v of NaCMC were increased.

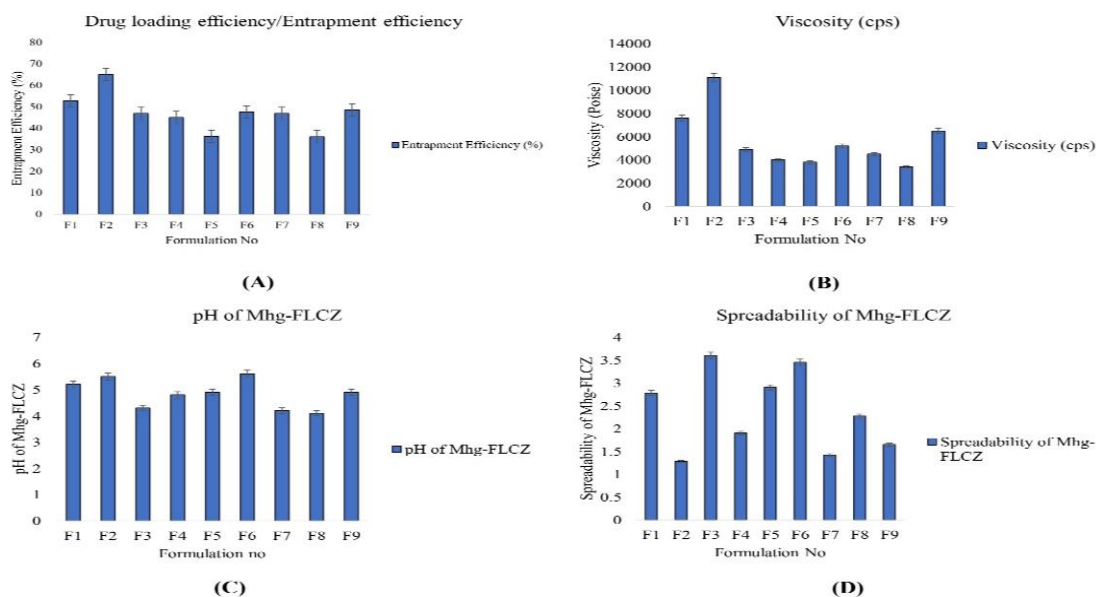


Fig. 4: (A) Bar diagrammatic representation of entrapment efficiency (EE%) of Mhg-FLCZ (mean \pm SD; n=6). (B) Bar diagrammatic representation of viscosity (cps) of Mhg-FLCZ (mean \pm SD; n=6). (C) Bar diagrammatic representation of pH of Mhg-FLCZ (mean \pm SD; n=6). (D) Bar diagrammatic representation of spreadability of Mhg-FLCZ (mean \pm SD; n=6)

Table 4: Evaluation parameters of Mhg-FLCZ

Formulation code	pH*	Spreadability*
F1	5.2 \pm 0.19	2.78 \pm 0.02
F2	5.5 \pm 0.24	1.28 \pm 0.04
F3	4.3 \pm 0.44	3.6 \pm 0.01
F4	4.8 \pm 0.54	1.9 \pm 0.01
F5	4.9 \pm 0.16	2.9 \pm 0.04
F6	5.6 \pm 0.28	3.45 \pm 0.06
F7	4.2 \pm 0.10	1.42 \pm 0.02
F8	4.1 \pm 0.18	2.27 \pm 0.06
F9	4.9 \pm 0.31	1.65 \pm 0.08

*mean \pm SD; n= 6

FT-TR (Fourier transform infrared)

Fig. 5(A) demonstrates that the IR of fluconazole exhibits absorption peaks at 3112.48 cm^{-1} for stretching of the -OH group, 1510.54 cm^{-1} for stretching of the triazole ring, 1111.96 cm^{-1} for bending of the C-F chain, 1361.07 cm^{-1} for bending of the phenyl-OH group, 1728.91 cm^{-1} for bending of the C=O chain, and 912.28 cm^{-1} for stretching of the C-C chain.

Fig. 5(B) shows that IR of fluconazole and polymer given a peak at 3113.35 cm^{-1} , 1510.39 cm^{-1} , 1111.79 cm^{-1} , 1361.24 cm^{-1} , 1729.71 cm^{-1} , 912.18 cm^{-1} for -OH stretching, triazole ring stretching, C-F bending, -OH bending of phenyl, C=O bending, and C-C stretching respectively. As a result of the stretching and bending of all peaks, it was determined that there was no molecular interaction between the drug and polymers because of the persistence of their internal structural and geometric configurations.

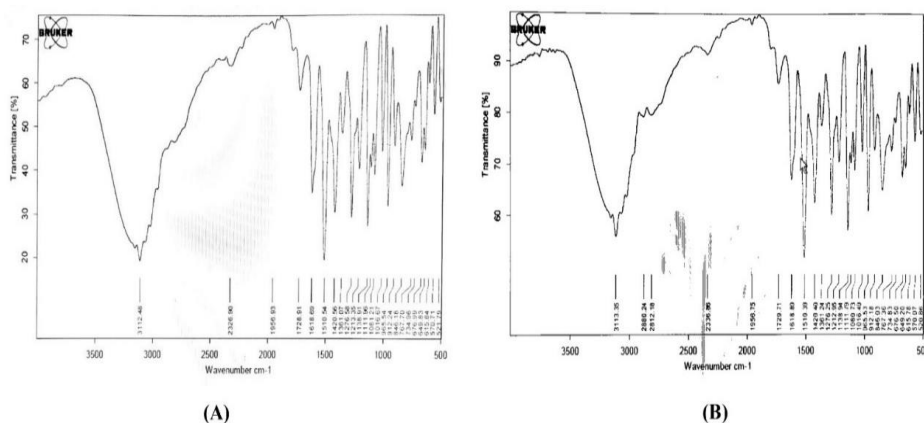


Fig. 5: (A) FT-IR spectra of FLCZ. (B) FT-IR spectra of FLCZ and polymers

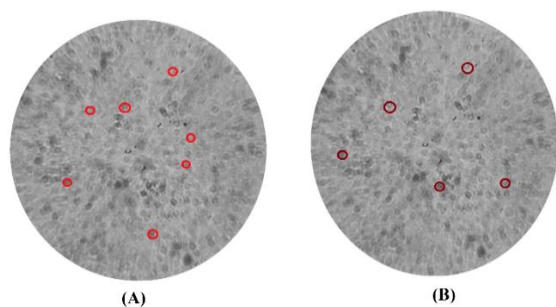


Fig. 6: (A) Visualize the particles of optimized batch (F2) Mhg-FLCZ using a binocular microscope at 1000X magnification. (B) Visualize the particles of optimized batch (F2) Mhg-FLCZ using a binocular microscope at 1500X magnification

Visual examination of Mhg-FLCZ

Fig. 6 illustrates the analysis of the binocular microscope (Labomed LX-300) visualizes the image at 1000X and 1500X magnification and

exhibits the Mhg-FLCZ's (Optimized F2 formulation) morphological characteristics. The topographical study confirmed that particles of Mhg-FLCZ (Optimized F2 formulation) were smooth surfaces spherical in nature.

In vitro dissolution study

The *in vitro* release profile of fluconazole from different gel formulations of Mhg-FLCZ is presented in fig. 7. The *in vitro* release profile demonstrated a significant ($p < 0.05$) increment of fluconazole release from gel containing Mhg-FLCZ. Release of the drug from Mhg-FLCZ impacts due to the amount of polymeric concentration and surfactant viscosity. The release of fluconazole was found significantly ($p < 0.05$) increased as the amount of CP was increased. The amount of drug released after 8 h was 56.82% (F1), 93.22% (F2), 77.86% (F3), 65.88% (F4), 43.67% (F5), 70.60% (F6), 60.22% (F7), 78.82% (F8) and 72.04% (F9). These unprecedented results prove the potential of fluconazole gel to increase fluconazole release through the prolonged delivery of fluconazole. The Mhg-FLCZ formulations can be ranked in the following order: F2 > F8 > F3 > F9 > F6 > F4 > F7 > F1 > F5. Formulation F2 containing 1.5% w/v of CP and 1.5% w/v of NaCMC showed the highest percentage of drug released as 93.22% within 8 h of *in vitro* analysis.

Table 4: In vitro release (%) of Mhg-FLCZ

Time (h)	F1	F2	F3	F4	F5	F6	F7	F8	F9
1	13.94	13.94	13.94	13.94	13.94	13.94	13.94	13.94	13.94
2	25.77	46.75	30.41	22.37	15.59	31.67	22.00	26.60	26.14
3	30.72	57.94	39.60	30.38	27.19	36.96	28.71	36.02	30.75
4	36.24	70.37	46.80	39.60	33.50	43.14	33.65	39.91	36.62
5	42.69	80.40	54.18	46.92	37.77	49.04	40.30	44.36	49.39
6	48.74	86.93	58.94	53.81	40.71	54.78	49.38	50.18	54.44
7	51.86	89.22	70.09	58.27	42.26	57.74	54.44	62.05	62.10
8	56.82	93.22	77.86	65.88	43.67	70.60	60.22	78.82	72.04

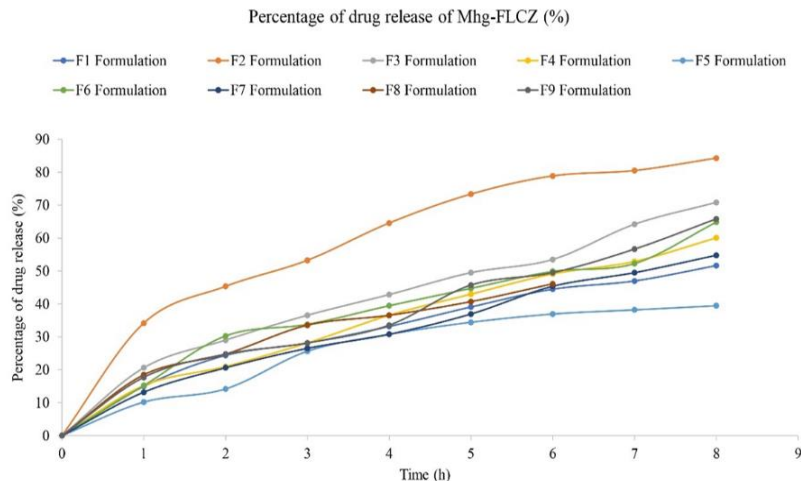


Fig. 7: Percentage of drug release of Mhg-FLCZ (F9 showed the highest percentage of drug release (93.22%))

Kinetic analysis of release data

The Mhg-FLCZ formulations' *in vitro* FLCZ release data has been represented using a variety of kinetic models. Table 5 displays the correlation coefficient (R^2) value after release data was fitted to multiple kinetic models and release processes. According to the highest correlation coefficient (R^2), the Higuchi equation (0.9762) was followed by zero-order kinetics (0.9858) in the release patterns of F2 formulation Mhg-FLCZ.

Optimization of Mhg-FLCZ by 3^2 factorial design

The polynomial equations for the independent and response variables were used to optimize for all three answers in order to find the best formulation. After trading off several answer factors, the following

acceptable response ranges have to be limited: Viscosity (cps) is 11100 ± 1.21 ; entrapment efficiency (%) is 65.09 ± 0.41 ; and drug release at 8 h (%) was 93.22%. It was determined, by a thorough analysis of the possibility search and subsequent grid studies, that the formulation comprising 1.5% w/v of CP and 1.5% w/v of NaCMC satisfies all requirements.

The produced Mhg-FLCZ formulation of F2 had an 8-hour drug release of 93.22% and an entrapment efficiency of 65.09 ± 0.41 %. Based on the aforementioned results, formulation F2 was found to be an optimized formulation. By using *design expert* trial version 13 software, optimized Mhg-FLCZ was selected for the F2 formulation because its lack of error (22.89) for the response of the dependent variables was the lowest of all comparisons with other formulations.

Table 5: A regression coefficient (R²) for the Mhg-FLCZ gel based on kinetics data analysis

F. No.	Zero-order kinetics (R ²)	First-order kinetics (R ²)	Higuchi plot (R ²)	Korsmeyer peppas model	
				R ²	n value
F1	0.9784	0.9552	0.9798	0.1398	1.4769
F2	0.9858	0.9476	0.9762	0.1303	1.4698
F3	0.963	0.9089	0.9858	0.1679	1.4628
F4	0.9538	0.9063	0.9761	0.1781	1.4575
F5	0.9821	0.9797	0.982	0.1516	1.4598
F6	0.9823	0.9728	0.983	0.1492	1.4559
F7	0.9851	0.9762	0.9763	0.1583	1.4468
F8	0.982	0.9781	0.9852	0.1461	1.4718
F9	0.9638	0.9541	0.974	0.1781	1.4743

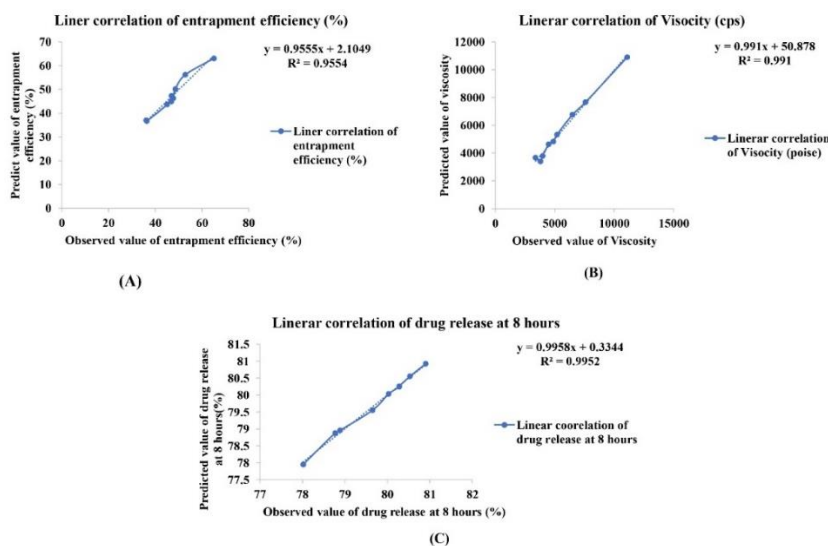


Fig. 8: (A) Graph of the linear relationship that exists between the actual and expected entrapment efficiency (%). (B) Graph of the linear relationship that exists between the actual and expected to viscosity (cps). (C) Graph of the linear relationship that exists between the actual and expected values for drug release at 8 h (%)

Table 6: Ex-vivo skin permeation study from Mhg-FLCZ

Time (h)	Absorbance	Dilution factor	Flux ($\mu\text{g}/\text{cm}^2/\text{h}$)	% Drug permeability*
1	0.164	10	0.563	20.60 \pm 0.54
2	0.247	10	0.541	31.03 \pm 0.32
3	0.347	10	0.550	43.59 \pm 0.21
4	0.394	10	0.531	49.50 \pm 0.41
5	0.469	10	0.522	58.92 \pm 0.47
6	0.564	10	0.510	70.85 \pm 0.57
7	0.597	10	0.510	84.67 \pm 0.26
8	0.674	10	0.510	84.67 \pm 0.67

*mean \pm SD; n= 6

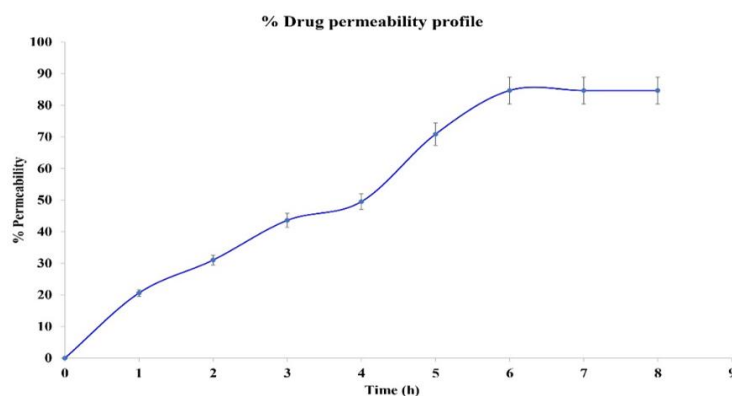


Fig. 9: Optimized Mhg-FLCZ (F2) percentage drug permeability of ex vivo permeation study

Ex-vivo permeation study

The Mhg-FLCZ gel exhibited $84.67 \pm 0.67\%$ in an 8-hour percentage drug permeability (%) in the *ex-vivo* permeation testing mentioned in table no 6. Percutaneous skin permeation analysis is impacted by using the Mhg-FLCZ formulation since it has a considerably more prominent controlled release pattern and is more efficient. The *Ex-vivo* drug permeation study revealed that the developed formulation showed excellent drug permeation through the skin.

The flux was calculated by using the equation of $J_{ss} = (dQ/dt)_{ss} \times 1/A$, where J_{ss} is the Steady State permeation flux ($\mu\text{g}/\text{cm}^2/\text{h}$), A is the area (cm^2) of skin membrane uncovered to the Franz diffusion cell, and $(dQ/dt)_{ss}$ is the permeated drug amount across the excised rat abdominal skin membrane per unit time at the steady state condition ($\mu\text{g}/\text{h}$).

Statistical analysis

The data obtained for different formulations was analyzed by one-way ANOVA. The values were considered to be statistically significant when the P value ≤ 0.05 . It was observed that the P value of all responses for the linear model was found to be ≤ 0.05 . Hence, the result obtained is considered as significant.

CONCLUSION

The results indicate that under optimized conditions, fluconazole can be successfully incorporated into a microemulsion gel system using topically acceptable surfactants, co-surfactants, and oil phases. The micro-emulsified hydrogel of fluconazole shows excellent entrapment efficiency, spreadability, and viscosity. Based on the physicochemical properties, *in vitro* and *ex-vivo* studies it was observed that developed fluconazole micro-emulsified gel formulation showed all acceptable ranges, controlled drug release profiles, and enhanced drug permeability. Therefore, it can be concluded that micro-emulsified hydrogel containing fluconazole has a potential application in topical delivery.

ACKNOWLEDGMENT

The authors are thankful to the Bengal School of Technology, Chinsurah, Hooghly, West Bengal, India, for providing the instruments, e-library facility, and adequate facilities to perform this experiment. The authors also express gratitude to Dr. P Suresh, Principal of Bengal School of Technology, Chinsurah, Hooghly, West Bengal, India, for invaluable support, guidance, motivation, and inspiration, which significantly contributed to this research.

FUNDING

Nil

AUTHORS CONTRIBUTIONS

Soumyadip Ghosh and Ankita Basak made significant contributions to preparing formulation strategies and evaluating individual parameters. Soumyadip Ghosh framed the manuscript, Ankita Basak and Debogopal Ganguly made corrections and revisions and did a literature survey for this research. Ankita Porey collected all the data and interpreted graphs. All authors contributed equally.

CONFLICT OF INTERESTS

No conflict of interest

REFERENCES

- Hamza MY, Abd El Aziz ZR, Aly Kassem M, El-Nabarawi MA. Loxoprofen nanosponges: formulation, characterization and *ex-vivo* study. *Int J App Pharm.* 2022;14(2):233-41. doi: 10.22159/ijap.2022v14i2.43670.
- Tiwari A, Tiwari A, Sharma S. Wound healing potential of acacia catechu in excision wound model using *in vitro* and *in vivo* approach. *Int J Pharm Pharm Sci.* 2023;15(12):27-36. doi: 10.22159/ijpps.2023v15i12.49539.
- Kumbhar MD, Karpe MS, Kadam VJ. Development and characterization of water-in-oil microemulsion for transdermal delivery of eperisone hydrochloride. *ACCTRA.* 2020;7(1):45-64. doi: 10.2174/2213476X06666190318120522.
- Eziuzo OS, Amarauche C. Studies on sida acuta hydrogel i: processing and physicochemical properties of the derived hydrogel obtained from south east nigeria. *Int J Pharm Pharm Sci.* 2017;9(6):5-11. doi: 10.22159/ijpps.2017v9i6.10097.
- Kumaran P, Gupta A, Sharma S. Synthesis of wound-healing keratin hydrogels using chicken feathers proteins and its properties. *Int J Pharm Pharm Sci.* 2017;9(2):171-8. doi: 10.22159/ijpps.2017v9i2.15620.
- Ahmed AB, Ahmed R, Sengupta R. Formulation and *in vitro/ex-vivo* characterizations of microemulsion-based hydrogel formulation of aceclofenac for topical application. *Asian J Pharm Clin Res.* 2016;9(7):87-91.
- Alam A, Mustafa G, Agrawal GP, Hashmi S, Khan RA, Aba Alkhayl FF. A microemulsion-based gel of isotretinoin and erythromycin estolate for the management of acne. *J Drug Deliv Sci Technol.* 2022;71:103277. doi: 10.1016/j.jddst.2022.103277.
- Maziad NA, El-hamouly S, Zied E, El Kelani AT, Rabie Nasef N. Radiation preparation of smart hydrogel has antimicrobial properties for controlled release of ciprofloxacin in drug delivery systems. *Asian J Pharm Clin Res.* 2015;8(3):193-200.
- Kajbafvala A, Salabat A. Microemulsion and microemulsion gel formulation for transdermal delivery of rutin: optimization, *in vitro/ex-vivo* evaluation and SPF determination. *J Dispers Sci Technol.* 2022;43(12):1848-57. doi: 10.1080/01932691.2021.1880928.
- Ibrahim TM, Ayoub MM, El-Bassossy HM, El-Nahas HM, Gomaa E. Investigation of alogliptin-loaded in situ gel implants by 2³ factorial design with glycemic assessment in rats. *Pharmaceutics.* 2022;14(9):1867. doi: 10.3390/pharmaceutics14091867, PMID 36145615.
- Nagam SP, Jyothi AN, Poojitha J, Aruna S, Nadendra RR. A comprehensive review on hydrogels. *Int J Curr PharmSci.* 2016;8(1):19-23.
- Chaerunisaa AY, Muhaimin. Comparative study on the release of two drugs in fixed-dose combination using zero order and first derivative spectrophotometry. *Int J PharmTech Res.* 2016;9(12):581-90.
- Scamoroscenco C, Teodorescu M, Burlacu SG, Gifu IC, Mihaescu CI, Petcu C. Synergistic antioxidant activity and enhanced stability of curcumin encapsulated in vegetal oil-based microemulsion and gel microemulsions. *Antioxidants (Basel).* 2022;11(5):854. doi: 10.3390/antiox11050854, PMID 35624718.
- Cui T, Yu J, Wang CF, Chen S, Li Q, Guo K. Micro-gel ensembles for accelerated healing of chronic wound via pH regulation. *Adv Sci (Weinh).* 2022;9(22):e2201254. doi: 10.1002/advs.202201254, PMID 35596608.
- Mehanna MM, Abla KK, Domiati S, Elmaradny H. Superiority of microemulsion-based hydrogel for non-steroidal anti-inflammatory drug transdermal delivery: a comparative safety and anti-nociceptive efficacy study. *Int J Pharm.* 2022;622:121830. doi: 10.1016/j.ijpharm.2022.121830, PMID 35589005.
- Malli K, Kumar L, Verma R. Felodipine-review of analytical methods developed for pharmaceutical dosage forms and biological fluids. *Int J App Pharm.* 2023;15(6):53-9. doi: 10.22159/ijap.2023v15i6.49211.
- Thombre NA, Niphade PS, D Ahire E, J Kshirsagar S. Formulation development and evaluation of microemulsion based lornoxicam gel. *Biosci Biotech Res Asia.* 2022;19(1):69-80. doi: 10.13005/bbra/2968.
- Ivanovski V, Shapovalova OE, Drozdov AS. Structural rearrangements of carbonic anhydrase entrapped in sol-gel magnetite determined by ATR-FTIR spectroscopy. *Int J Mol Sci.* 2022;23(11):5975. doi: 10.3390/ijms23115975, PMID 35682654.
- Hajjar B, Zuo J, Park C, Azarmi S, Silva DA, Bou-Chacra NA. *In vitro* evaluation of a foamable microemulsion towards an improved topical delivery of diclofenac sodium. *AAPS PharmSciTech.* 2022;23(4):102. doi: 10.1208/s12249-022-02258-0, PMID 35378669.
- Abla KK, Domiati S, El Majzoub R, Mehanna MM. Propranolol-loaded limonene-based microemulsion thermo-responsive mucoadhesive nasal nanogel: design, *in vitro* assessment, *ex vivo*

- permeation, and brain biodistribution. *Gels*. 2023;9(6):491. doi: 10.3390/gels9060491, PMID 37367161.
21. Shankar VK, Wang M, Ajarapu S, Kolimi P, Avula B, Murthy R. Analysis of Docosanol using GC/MS: method development, validation, and application to ex vivo human skin permeation studies. *J Pharm Anal*. 2022 Apr 1;12(2):287-92. doi: 10.1016/j.jpha.2021.08.004, PMID 35582396.
 22. Ferrara F, Benedusi M, Cervellati F, Sguizzato M, Montesi L, Bondi A. Dimethyl fumarate-loaded transethosomes: a formulative study and preliminary ex vivo and *in vivo* evaluation. *Int J Mol Sci*. 2022;23(15):8756. doi: 10.3390/ijms23158756, PMID 35955900.
 23. Soriano Meseguer S, Fuguet E, Port A, Roses M. Suitability of skin-PAMPA and chromatographic systems to emulate skin permeation. Influence of pH on skin-PAMPA permeability. *Microchem J*. 2023;190:108567. doi: 10.1016/j.microc.2023.108567.
 24. Lynch B, Pagon H, Le Blay H, Brizion S, Bastien P, Bornschlöggl T. A mechanistic view on the aging human skin through ex vivo layer-by-layer analysis of mechanics and microstructure of facial and mammary dermis. *Sci Rep*. 2022;12(1):849. doi: 10.1038/s41598-022-04767-1, PMID 35039567.
 25. Nawaz A, Farid A, Safdar M, Latif MS, Ghazanfar S, Akhtar N. Formulation development and ex-vivo permeability of curcumin hydrogels under the influence of natural chemical enhancers. *Gels*. 2022;8(6):384. doi: 10.3390/Gels8060384, PMID 35735728.
 26. Thakkar HP, Savsani H, Kumar P. Ethosomal hydrogel of raloxifene HCl: statistical optimization & ex vivo permeability evaluation across microporated pig ear skin. *Curr Drug Deliv*. 2016;13(7):1111-22. doi: 10.2174/1567201813666160120151816, PMID 26787414.
 27. Rapalli VK, Sharma S, Roy A, Alexander A, Singhvi G. Solid lipid nanocarriers embedded hydrogel for topical delivery of apremilast: *in vitro*, ex-vivo, dermatopharmacokinetic and anti-psoriatic evaluation. *J Drug Deliv Sci Technol*. 2021;63:102442. doi: 10.1016/j.jddst.2021.102442.
 28. Abrego G, Alvarado H, Souto EB, Guevara B, Bellowa LH, Garduno ML. Biopharmaceutical profile of hydrogels containing pranoprofen-loaded plga nanoparticles for skin administration: *in vitro*, ex vivo and *in vivo* characterization. *Int J Pharm*. 2016;501(1-2):350-61. doi: 10.1016/j.ijpharm.2016.01.071, PMID 26844786.
 29. Jagadeesh K, Kadiyala KG, Varma Dendukuri BNS, Guttula RS, Gupta Tiruveedhi VLNB, Vamsi P. Quality control assessment of dutasteride and silodosin in capsules and tablets employing a novel developed HPLC technique; evaluation of stabilities of dutasteride and silodosin in accelerated degradation. *Int J App Pharm*. 2023;15(6):98-107. doi: 10.22159/Ijap.2023v15i6.49036.
 30. Khalifa MY, Shaikh Siraj N. Formulation and characterization of floating beads of antibiotic by emulsion gelation technique. *Asian J Pharm Clin Res*. 2019;12(5):57-62. doi: 10.22159/ajpcr.2019.v12i5.32103.
 31. KR, Biju PS, Aggarwal Nn, VS, Rai D. Development of aceclofenac loaded microsponge gels: a statistical quality by design (qbd) approach towards optimization and evaluation. *Int J Appl Pharm*. 2023;15(6):178-87. doi: 10.22159/Ijap.2023v15i6.49122.
 32. UG, Patil A, GH. Formulation and evaluation of nanoparticle drug delivery system for treatment of hypertension. *Int J App Pharm*. 2023;15(6):90-7. doi: 10.22159/Ijap.2023v15i6.48971.
 33. Narayanankutty Anjana M, Kumar M, BS V, M Mathews S, Kumar KPS. Development and assessment of the cilostazol solid dispersion employing melt and solvent evaporation method and its comparison. *Int J App Pharm*. 2023;15(6):222-8. doi: 10.22159/Ijap.2023v15i6.48090.